ARMY RESEARCH LABORATORY

Surface Characterization of Cu-ion Implanted Single Crystal and Thin Film ZnO for Catalytic Applications

J.S. Brodkin and D. Chadwick

ARL-TR-752

May 1995

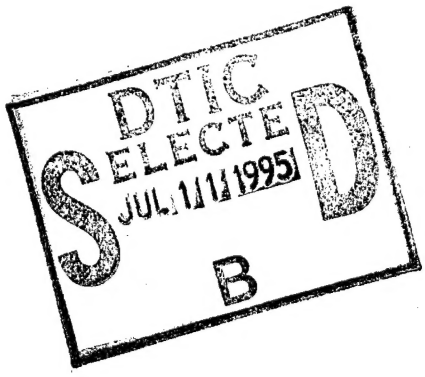

The findings in this report are not to be construed as an official Department of the Army position unless so designated by other authorized documents.

Citation of manufacturer's or trade names does not constitute an official endorsement or approval of the use thereof.

Destroy this report when it is no longer needed. Do not return it to the originator.

REPORT DOCUMENTATION PAGE

Form Approved
OMB No. 0704-0188

1. AGENCY USE ONLY *(Leave blank)*	2. REPORT DATE	3. REPORT TYPE AND DATES COVERED
	May 1995	Sum. 9/6/92 - 9/3/93

4. TITLE AND SUBTITLE
Surface Characterization of Cu-ion Implanted Single Crystal and Thin Film ZnO for Catalytic Applications

5. FUNDING NUMBERS

6. AUTHOR(S)
J.S. Brodkin and *D. Chadwick

7. PERFORMING ORGANIZATION NAME(S) AND ADDRESS(ES)
Army Research Laboratory
Watertown, MA 02172-0001
ATTN: AMSRL-MA-CC

8. PERFORMING ORGANIZATION REPORT NUMBER
ARL-TR-752

9. SPONSORING/MONITORING AGENCY NAME(S) AND ADDRESS(ES)

10. SPONSORING/MONITORING AGENCY REPORT NUMBER

11. SUPPLEMENTARY NOTES
*D. Chadwick, Imperial College of Science, Technology and Medicine

12a. DISTRIBUTION/AVAILABILITY STATEMENT
Approved for public release; distribution unlimited.

12b. DISTRIBUTION CODE

13. ABSTRACT *(Maximum 200 words)*

Single crystals and thin films of zinc oxide were implanted with copper ions in order to study the catalytic properties of a mixed Cu-ZnO system. ZnO is widely used as a catalyst in the methanol synthesis reaction, and copper has been noted to have a synergistic effect on the rates and yields of reaction. The samples were characterized by x-ray photoelectron spectroscopy (XPS) before and after implantation, and surface copper concentration in the implanted specimens was determined. Implanted samples were heated under oxidizing and reducing atmospheres and re-examined by XPS to determine the oxidation state of the implanted copper species. XPS results demonstrated that the oxidation state of the copper could be manipulated, although there was a corresponding decrease in the concentration of the surface copper ions, relative to temperature and time of heating.

14. SUBJECT TERMS
Surface Analysis, Catalysis, Zinc Oxide, XPS

15. NUMBER OF PAGES
15

16. PRICE CODE

17. SECURITY CLASSIFICATION OF REPORT	18. SECURITY CLASSIFICATION OF THIS PAGE	19. SECURITY CLASSIFICATION OF ABSTRACT	20. LIMITATION OF ABSTRACT
Unclassified	Unclassified	Unclassified	UL

NSN 7540-01-280-5500

Standard Form 298 (Rev. 2-89)
Prescribed by ANSI Std. Z39-18
298-102

Surface Characterization of Cu-ion Implanted Single Crystal and Thin Film ZnO for Catalytic Applications

J.S. Brodkin, U.S. Army Research Laboratory, Materials Directorate (Metals Research Branch) and D. Chadwick, Imperial College of Science, Technology and Medicine (Department of Chemical Engineering and Chemical Technology).

INTRODUCTION

During the period of September 1992 - September 1993 a joint project was carried out by personnel of the two laboratories noted above, at Imperial College, London, England. The work was conducted in the Department of Chemical Engineering in the sub-group of Applied Catalysis and Reaction Engineering.

This group's work focuses on the use of catalysis and high temperature pyrolysis for energy and fuel related processes, in particular methanol synthesis. The catalytic synthesis of alcohols and oxygenates is a currently important research area due to the increasing usage of oxygenates as potential transportation fuels and as octane enhancers in unleaded gasoline [1].

However, the field has been well-studied for many years. In the early 1960's a ground-breaking study by researchers at ICI led to the development of a copper-zinc oxide catalyst which enabled methanol to be synthesized under much milder conditions than were previously used, and this process is still widely used today [2]. However, many fundamental aspects of the mechanisms of these reactions are still poorly understood. One of the main aims of this research program has been to determine the detailed mechanisms of these synthesis reactions by investigation of the kinetics of these systems. This has been carried out using high pressure, micro-reactor techniques, followed by surface characterization of the catalysts under ultrahigh vacuum.

The particular project of interest during this one-year period was the investigation of single crystal ZnO which had been ion-implanted with ^{63}Cu, and was to be a model system for the study of the Cu/ZnO based catalyst for the industrial process. In industry the catalyst is a physical mixture of microcrystalline ZnO and finely ground Cu metal. In the commercial reactor, the reaction gases CO, CO_2 and H_2 (a mixture commonly referred to as syngas) are passed over the catalytic mixture at conditions of elevated temperature and pressure (T = 250° C, p = 10 bar):

$$CO + CO_2 + 5\ H_2 \xrightarrow{ZnO/Cu} 2\ CH_3OH + H_2O$$

The Zn and the Cu are believed to have a synergistic effect and to result in a greatly enhanced catalytic activity, relative to what can be achieved by the use of ZnO alone [3].

The use of ion implantation to produce a mixed Zn-Cu system was proposed in order to allow careful study of what occurs in the catalyst under reaction conditions, with a material which was carefully controlled in terms of concentration and purity of the components. The same reaction mixture used in the industrial reactors was prepared in a small high pressure gas cell which was then linked to a surface characterization instrument, all under ultrahigh vacuum and isolated from atmospheric conditions. Therefore, after completion of the synthesis reaction the catalyst could be directly examined in order to determine the surface active species.

Previous studies attempted to explain the mechanism of the reaction, and many possiblities have been proposed, as discussed in an important review of methanol synthesis published by Klier [4]. Herman et al. proposed a model of Cu^+ dissolved in ZnO as the active center for methanol synthesis [5] in the first piece of work that applied modern surface science techniques to the study of the catalysts used in these reactions. In contrast to this view of the synergistic effect between Cu and ZnO, it has also been suggested that the ZnO acts merely as a structural support for the Cu catalyst and takes no part in the mechanism of the reaction [6]. Finally, the ICI research group has recently proposed that it is metallic copper that is the main active center in the synthesis [7].

In the current study, we were especially interested in the oxidation state of the Cu species, with a view towards settling the question of whether it is Cu^0 or Cu^+ which acts as the active center, and at what Cu concentration we might expect to find enhanced reactivity. The first objective of this project was to implant a variety of materials with ^{63}Cu ions, including single crystal ZnO, polycrystalline ZnO on Zn foil or metal, and MgO crystals. When ion implantation of the substrate materials was completed, surface characterization of the implanted specimens was carried out in order to determine the surface concentration of Cu and its oxidation state. The final objective of the project was to be the processing of the implanted catalysts under reaction conditions, and the study of the altered surface state of the Cu/ZnO catalyst.

EXPERIMENTAL

Highly pure single crystals of ZnO in the needle formation were obtained and used in this study. The end faces of the crystals are hexagons about 1 mm wide, while the long axes of the crystals varied from about 5 to 15 mm long. A second potential catalyst material which is also of interest, MgO, was included in this study. The MgO specimens were obtained from a single crystal of MgO in a square rod formation using a diamond wafering saw and cut perpendicular to the long axis along the cleavage planes. Each MgO sample thus obtained was a square plate approximately 5 x 5 x 2 mm thick. The Zn foil was obtained from the Royal School of Mines and oxidized at 350° C for four hours under a stream of air. The resultant ZnO films were straw colored.

The samples were implanted with ^{63}Cu ions using a Whickham Ion Implanter which was located in the Electrical Engineering Department of Imperial College. There were two implantation runs: the first in 1988, which resulted in four ZnO single crystals implanted with ^{63}Cu at a dose of 1 x 10^{16} ions/cm^2, and a second run in 1993 with a greater variety of specimens and doses. In both implantations the beam energy was 50 keV with an average beam current of 100 μA/cm^2. Figure 1 illustrates the implantation set-up conditions for these two runs.

In the more recent implantation four different doses were attained. The highest dose was 1 x 10^{16} ions/cm^2 which was delivered to six ZnO crystals, two MgO crystals and two ZnO/Zn foil samples. A lower dose of 5 x 10^{15} ions/cm^2 was delivered to seven ZnO crystals, two MgO crystals and two ZnO/Zn foil samples. Two additional lower doses were delivered to some additional specimens. The samples were adhered to four pieces of silicon wafer using a silver soldering paste. The wafers were mounted onto a square plate, as shown in Figure 2, and attached to an x-y translation stage which was fitted inside the implanting chamber. As the desired dose was achieved, the specimens were moved out of the beam line.

X-ray photoelectron spectroscopy (XPS) was conducted on a Vacuum Generators Escalab Mark II, at pressures of around 2 x 10^{-9} mbar. The pass energy was 50 eV for all runs. The survey scan area was taken from 1200 to 0 eV, and the elemental scans were taken in ranges of 20-25 eV. Both the Mg (λ = 1253.6 eV) and Al (λ=1486.6 eV) anodes were utilized.

The high pressure studies were carried out in a Vacuum Generators high pressure gas cell which was located in the fast entry load lock of the Escalab Mark II. Some samples were heated on a P-8 resistive heater located in the preparation chamber of the Mark II. Several samples were

sputtered with an Ar ion gun which was also located in the preparation chamber. Ion Scattering Spectroscopy (ISS) was carried out on a few of the samples. Figure 3 shows the schematic representation of the UHV dual chamber XPS system used in these experiments.

The Rutherford Backscattering Spectroscopy (RBS) measurements were conducted at the ARL surface characterization facility at Watertown, MA. A single crystal of ^{63}Cu-implanted ZnO from the 1988 implantation at Imperial College was mounted on a piece of silicon wafer in a vacuum chamber and exposed to a beam of 2 MeV He^+ ions. The angle of incidence of the beam was 60° and the backscattering angle was 170°. Atomic fractions of the surface elements were deduced from a RUMP [8,9] fit to the RBS spectrum.

RESULTS AND DISCUSSION

A total of 38 samples of ZnO and MgO single crystals and ZnO films on Zn foil were implanted with ^{63}Cu ions to the required doses. It was noted by the operator that the single crystals exhibited some color changes during the implantation procedure. The ZnO crystals glowed bright green from the beginning of the run, although the color faded and disappeared when the dose reached approximately 10^{14} ions/cm^2. The MgO crystals fluoresced pale blue from the beginning of the run until the dose reached about 10^{14} ions/cm^2; the color then changed to bright green and remained so for the rest of the implantation. This was not unexpected as both materials are photoluminescent.

A certain amount of sputtering of the sample surface during implantation is expected and the extent will vary depending upon implantation conditions and sample composition. In general, a low dose implantation results in less sputtering and leads to a "buried" implanted layer, while a high dose implantation causes more sputtering loss and results in a more uniformly distributed (from the surface) implanted layer. This is illustrated in Figure 4. This implantation profile is consistent with surface analysis data obtained on the ZnO single crystal (1988 high dose implantation). Data from the RBS experiment showed a copper concentration of 9.4 atomic % averaged over 482 Å while results from an XPS experiment on the same crystal indicated 10.6 atomic % copper in the near surface region of 50 Å.

There are a number of computer programs available which will model the effect of the ion beam upon the substrate material. These programs are used to approximate the amount of expected surface material loss and resulting impurity concentration

and distribution under various conditions of ion implantation. Using one such program, Profile [10], for the case of single crystal ZnO and assuming an original 30 Å layer of carbon on the crystal surface (carbon is a common and pervasive atmospheric contaminant), a dose of 10^{16} ions/cm^2 will result in all of the carbon being sputtered away. In addition, there will be less sputtering on the crystal face which is normal to the ion beam. Results from the modeling analyses indicate that there might be a maximum of 5% Cu ions implanted extending over a depth of 350-400 Å.

The MgO crystals were freshly cleaved and not expected to contain much surface carbon. The Profile calculations indicate that the highest dose of 10^{16} ions/cm^2 might result in a much lower concentration of Cu ions, with a maximum of only about 1% Cu in a surface region of 600 Å.

The primary method of characterization of the Cu-implanted crystals and foils was XPS. A survey scan was always run first in order to determine the extent of carbon contamination and to obtain a rough idea of the relative amounts of copper, zinc and oxygen present. After the survey scan, a number of detail scans were obtained in order to get better resolution and quantification of the individual elemental peaks of interest. Before any heating or treatment of the samples was initiated, an XPS experiment on each of the following specimens was conducted:

1. ZnO crystals- unimplanted.
2. ZnO crystals implanted 1988, dose = 1 x 10^{16} ions/cm^2.
3. ZnO crystals implanted 1993, dose = 1 x 10^{16} ions/cm^2.
4. MgO crystals implanted 1993, dose = 1 x 10^{16} ions/cm^2.
5. ZnO film on Zn foil implanted 1993, dose = 1 x 10^{16} ions/cm^2.
6. ZnO film on Zn foil implanted 1993, dose = 5 x 10^{15} ions/cm^2.

Because the XPS survey spectra for all of the ZnO samples are quite similar, a representative spectrum from the single crystal unimplanted ZnO is shown in Figure 5. The Zn 3p peak is at 90 eV and the Zn 3s peak is at 142.5 eV. The stronger signals are from the Zn $2p_{3/2}$ and Zn $2p_{1/2}$ binding energies, which are at 1023.5 and 1047 eV respectively. There are several Zn Auger lines in the region 300-350 eV (Mg Kα). Oxygen shows up as a strong signal due to the 1s binding energy at 533.8 eV with a corresponding Auger series at 725-785 eV (Mg Kα). There is a strong peak due to the carbon 1s binding energy at 287.5 eV, indicating a large amount of surface carbon present. Finally, there is a doublet at 27-29 eV which is due to the Ta 4f binding energies, and is present in the case of all the ZnO single crystal samples because the crystals are resting on a background of Ta foil.

The survey scan from the ^{63}Cu ion-implanted (1993) ZnO single crystal is shown in Figure 6. The Zn, O, Ta and C peaks are all in their expected locations, although the carbon peak is much reduced relative to the unimplanted crystal; apparently most of the carbon contamination was sputtered away during the implantation procedure. There is an additional peak due to the presence of the implanted copper ions. The Cu $2p_{3/2}$ peak is at approximately 933.6 eV (depending on the sample), but is quite weak due to the low concentration of Cu ions in the sample surface region, due to sputtering. The Auger lines which would be attributed to Cu are obscured by the strong Zn Auger lines in the same region.

The survey spectrum for the ^{63}Cu-implanted MgO single crystal is shown in Figure 7. There are several weak lines which can be attributed to the binding energies of the Mg 2p peak at 47 eV and the Mg 2s peak at 74.5 eV. There is a strong signal due to carbon at 287.5 eV and a strong oxygen signal at 532 eV. There is no apparent peak due to copper, and a subsequent elemental detail scan reveals no Cu 2p signal at all in the expected region. The conclusion is that the implanted copper ions must be quite deeply embedded in the crystal (relative to the 15Å escape depth) and so will not be able to be seen with XPS, unless the implanted layer is exposed by sputtering of the surface region. That was not done for the purposes of this study, and so the MgO crystals were not further characterized.

Representative elemental detail scans from the ZnO single crystal, 1993 implantation are shown in Figures 8-10. There are small shifts in position and differences in peak areas between the different specimens which will be discussed later. In Figure 8 is shown the detail scan for Zn $2p_{3/2}$ and Zn $2p_{1/2}$. In Figure 9 is the oxygen 1s detail, and in Figure 10 is shown the Cu $2p_{3/2}$ peak and the Cu $2p_{1/2}$ peak. Detail scans in the same regions were taken on each of the single crystal ZnO samples (both unimplanted and implanted) and on the ZnO film on Zn foil samples. Results are shown in Table 1.

Table 1. Peak Positions in Binding Energy (eV) for the XPS elemental scans for all the unimplanted and ^{63}Cu-implanted specimens. Also shown is the surface copper concentration for the implanted samples.

Sample	Zn $2p_{3/2}$, eV	O 1s, eV	C 1s, eV	Cu $2p_{3/2}$, eV	Cu, at. %
Unimplanted ZnO crystal	1024.1	533.8	287.2	---	---
Implanted 1988 ZnO crystal	1022.6	531.7	286.0	933.7	10.6 +/- .5
Implanted 1993 ZnO crystal	1022.6	531.6	285.7	933.7	4.4 +/- .4
Implanted 1993 ZnO film/Zn foil high dose	1022.6	531.9	286.0	933.8	1.4 +/- .2
Implanted 1993 ZnO film/Zn foil medium dose	1022.6	531.5	285.9	933.7	1.2 +/- .2

As can be seen from Table 1 there is not much shift in the peak positions of the elemental components in any of the single crystal ZnO or thin film ZnO. The shift in the C 1s position from the standardized 284.6 eV indicates a small amount of charging on most of the samples. The position of the Zn $2p_{3/2}$ peak is consistent with the presence of Zn^{2+} in ZnO. The position of the Cu $2p_{3/2}$ peak indicates the presence of either Cu^0 or Cu^{1+} (Cu^{2+} can be ruled out on the basis of peak position and by the absence of satellite peaks in the region of the detail scan). It is not possible to distinguish between Cu^0 and Cu^{1+} on the basis of the position of the $2p_{3/2}$ peak alone. In order to be able to determine if the oxidation state of the copper present is 0 or 1+, one must consider the position of the Auger lines assigned to the surface copper species. There will be more discussion on this topic later.

In terms of the concentration of the copper present, it should be noted that there is a significant difference in the percent copper present between the two implantations of the ZnO single crystals. One explanation might be that small differences in sample orientation of the crystal relative to the ion beam may result in differences in apparent dose due to ion channeling effects. Channeling can occur if implanted species are directed between lattice planes or along axes and therefore experience lower energy loss rates. This would

result in a longer range and hence lower concentrations of the implanted ions at the outermost sample surface.

The thin film ZnO on Zn foil samples exhibited a much lower concentration of Cu ions after the implantation than the single crystal specimens. Both the high dose and the medium dose foil samples were analyzed, but the copper concentrations in these specimens were so low that the even lower dose samples were not characterized, due to the limitations of the XPS techniques.

Because it was important to determine the true oxidation state of the implanted Cu ions, it was necessary to obtain spectra containing binding energies of the Cu Auger lines. This is because the positions of the Auger lines for copper will be shifted depending upon whether the Cu present is Cu^0 or Cu^{1+}. (The actual measurement of interest is known as the Auger parameter, which is the difference in binding energy between the photoelectron and Auger lines.) Unfortunately, in the case of the single crystal ZnO specimens, all Cu Auger lines were completely obscured by the Zn Auger lines, which were in the same region and are very much stronger. However, the XPS spectra of the Zn foil specimens did exhibit Cu Auger signals, and the positions of these peaks indicated that the implanted copper was Cu^0. This is shown in Figure 11.

Since it was now known that the copper present in the implanted ZnO foils was Cu^0 it was possible to carry on with the planned high pressure gas cell experiments. The objective of this part of the study was to determine if (a) the oxidation state of the copper could be adjusted depending upon reaction conditions, and (b) what would happen to the concentration of the implanted Cu ions as a result of heating and/or exposure to different reaction mixtures. The ultimate aim of these experiments would be to process the model catalyst under industrial conditions in order to determine the oxidation state and local environment of the copper ions. This would elucidate the mechanism of the catalytic reaction in terms of the role of the copper species.

We had planned to use the ZnO crystals as the principal materials of study but because it would not be possible to monitor the Cu Auger binding energies in these samples, we turned to the foil specimens as an alternative. However, the crystal specimens were used to determine proper reaction conditions and optimum gas mixtures and to get preliminary data on the reaction of the specimens under catalytic conditions. After suitable reaction conditions were determined, we planned to initiate a similar study using the foil samples.

At this point the ZnO crystals from the 1988 implantation at Imperial College were examined for a second time because in

the interim period they had been heated in nitrogen at 300°C. There were small changes in the survey spectrum, but the main difference noted was the decrease in concentration of copper in the surface region from 10.6 % to 7.5 %. After further heating in oxygen at 475° C it was noted that there was another large drop in the surface concentration of copper species. Heating in hydrogen at a lower temperature changed many of the peak positions but did not result in a further large drop in copper concentration. Heating the crystals at 475° C in hydrogen also resulted in the removal of virtually all of the surface carbon contamination. Results of this study are shown in Table 2 and in Figures 12 through 14.

As can be seen from Table 2 and in Figure 12, there is a small shift upwards in binding energy of the Cu $2p_{3/2}$ peak in the oxygen and heat-treated ZnO crystal (spectrum "b") relative to the spectrum of the untreated sample(spectrum "a"). This indicates oxidation of the implanted copper ions from the likely zero valence state to Cu^{2+}. After being heated in a hydrogen atmosphere, the Cu $2p_{3/2}$ signal shifts downward again (spectrum "c"), which is an indication that the the copper ions have been reduced to either Cu^0 or Cu^{1+}. This experiment clearly shows that the both the surface copper concentration and oxidation state of the copper ions can be manipulated by exposure to various atmospheres and temperatures.

Figure 13 shows the expanded region of the elemental copper binding energies for the untreated and treated ZnO crystals. Spectrum (a) is of the untreated zinc oxide crystal (Cu-implanted but not exposed to heat or oxygen, nitrogen, or hydrogen atmospheres). Spectrum (b) is of the same crystal after being heated in oxygen at 475° C. Spectrum (c) is of the same crystal after further heating in hydrogen at 220° C. The important feature to note here is the satellite peak in between the Cu $2p_{3/2}$ and the Cu $2p_{1/2}$ peaks in spectrum (b). This feature appears only when Cu^{2+} is present and is a clear indication that the implanted copper ions have been oxidized.

Figure 14 shows the XPS spectra for the same crystal after the same sequence of heating in various atmospheres for the detail scan of the O1s elemental region. In this case, the O1s peak does not shift significantly after oxidation, but does exhibit a small downward shift in binding energy after being heated in reducing atmosphere. The reason for this shift is not clear, but may be related to a different oxygen coordination due to the reduction of CuO to Cu_2O or Cu^0.

Table 2. Peak Positions in Binding Energy (eV) for the XPS elemental scans for the untreated and treated Cu-implanted ZnO crystals. Also shown is surface copper concentration.

Sample	Zn $2p_{3/2}$, eV	O 1s, eV	C 1s, eV	Cu $2p_{3/2}$, eV	Cu,at.%
Implanted 1988 ZnO, untreated	1022.6	531.7	286.0	933.7	10.6 +/- .5
N_2, 300° C, 1 hour	1022.7	531.9	285.9	933.7	7.5 +/- .6
O_2, 475° C, 2 hours	1022.1	531.9	---	934.1	4.3 +/- .8
H_2, 220° C, 2 hours	1022.4	531.5	---	933.3	4.1 +/- .6

CONCLUSIONS

The proposed project was successful insofar as a model material was produced and characterized, and could be used to demonstrate the catalytic properties and synergistic effects of a mixed Cu-ZnO system. There were some difficulties in using the Cu-implanted zinc oxide crystals as the model system due to the weakness of the copper Auger lines and the resultant ambiguity regarding the assignment of the Auger parameter in these materials. This problem could be circumvented by using the foil specimens instead which did allow determination of the oxidation state of the implanted copper species. It was clearly shown that the Cu oxidation state could be manipulated by exposure to various oxidizing and reducing atmospheres at elevated temperatures in the high pressure gas reaction cell of the Escalab Mark II. The work that remains to be done is the reaction of the foil specimens under true catalytic conditions followed by characterization of the implanted copper species.

ACKNOWLEDGEMENTS

The authors wish to thank Ms. Wendy Kosik for conducting the RBS experiment.

REFERENCES

1. W.O. Haag and J.C. Kuo, Chapter 5 in Energy **12** 1987, 689.

2. G. C. Chinchen, P. J. Denny, J. R. Jennings, M. S. Spencer and K. C. Waugh, Appl. Catal., 1988, **36**, 1.

3. R. Burch and R.J. Chappell, Appl. Catal., 1988, **45**, 131-150.

4. K. Klier, Adv. Catal., 1982, **31**, 243.

5. R. G. Herman, K. Klier, G. W. Simmons, B. P. Finn, J. B. Bulko and T. P. Kobylinski, J. Catal., 1979, **56**, 407.

6. G. C. Chinchen, K. C. Waugh and D. A. Whan, Appl. Catal. 1986, **25**, 101.

7. S. P. S. Andrew, 7th Int. Congr. Catal., Post Congr. Symp., Osaka, paper 12, 1980.

8. L. R. Doolittle, Nucl. Instrum. Meth. B, 9 (1985) 334.

9. L. R. Doolittle, Nucl. Instrum. Meth. B, 15 (1986) 227.

10. S. N. Bunker and A. J. Armini, Nucl. Instrum. and Meth. in Physics Res., B39 (1989) 7-10.

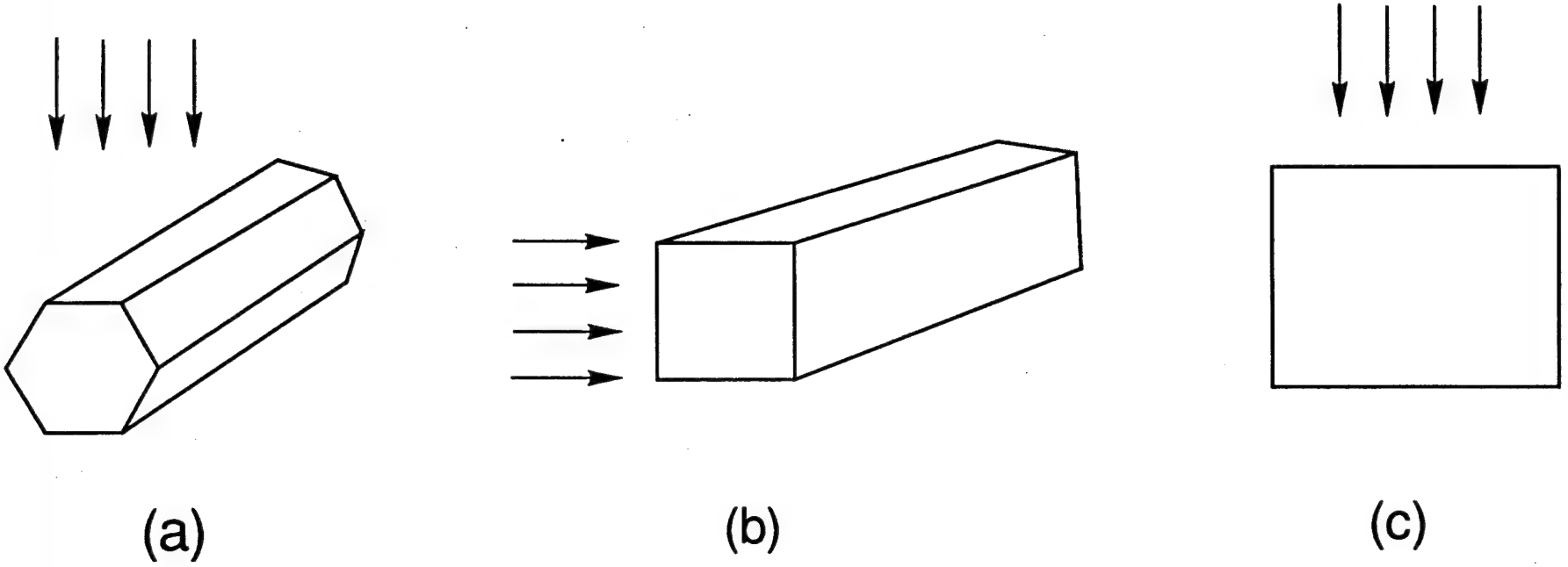

Figure 1.

Implantation of materials using a ^{63}Cu ion beam. (a) ZnO crystals were implanted with ^{63}Cu ions at 90° to the top long face and 30° to the side face. (b) MgO crystals were split along cleavage planes and implanted 90° to the front face of the cleavage plane. (c) ZnO thin films on Zn foil were implanted on the front face of the foil.

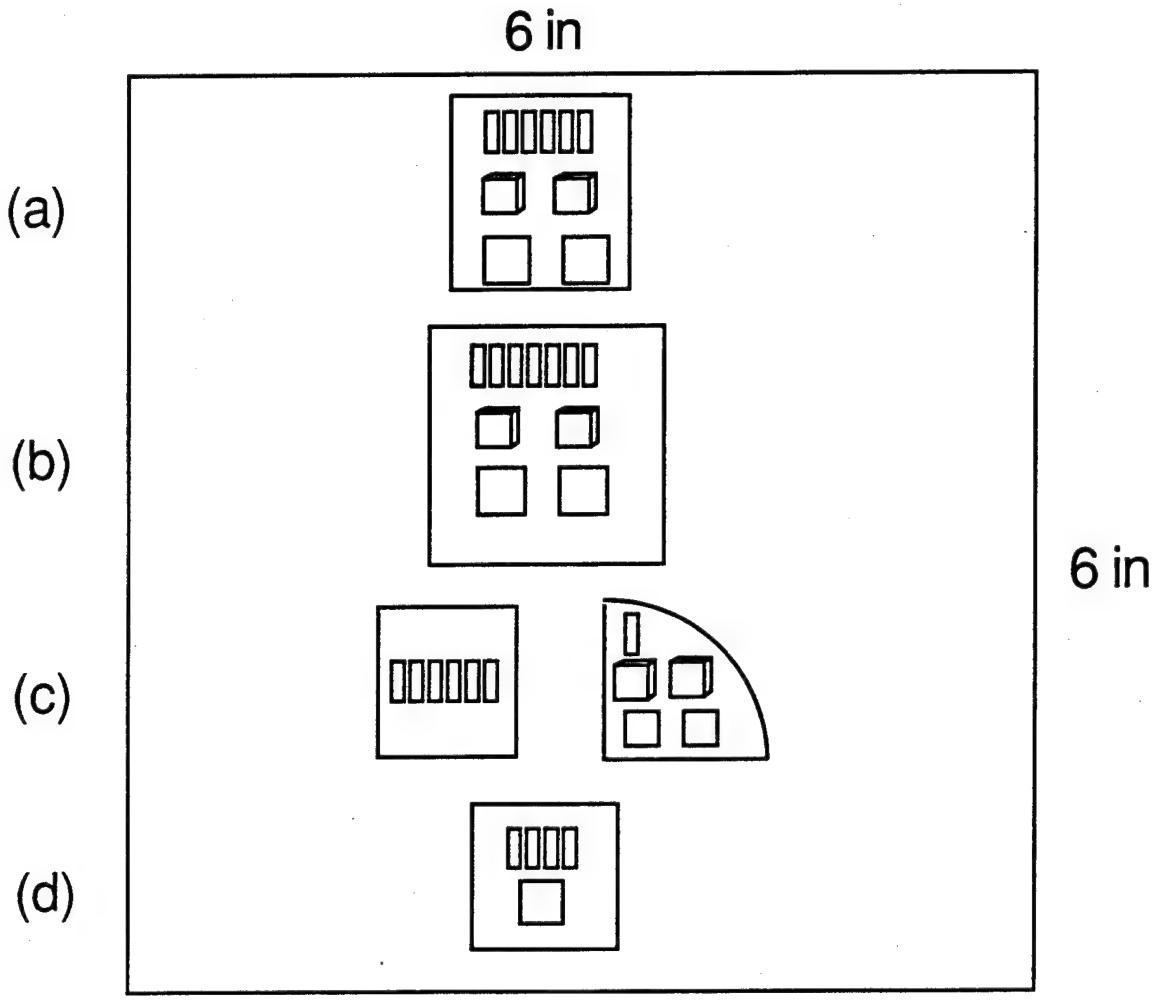

Figure 2.

Schematic representation of implanted specimens. (a) 6 ZnO crystals, 2 MgO crystals, 2 ZnO/Zn foil samples; dose = 1×10^{16} ions/cm^2 . (b) 7 ZnO crystals, 2 MgO crystals, 2 ZnO/Zn foil samples; dose = 5×10^{15} ions/cm^2 . (c) 7 ZnO crystals, 2 MgO crystals, 2 ZnO/Zn foil samples; dose = 2×10^{15} ions/cm^2 . (d) 4 ZnO crystals, 1 ZnO/Zn foil sample; dose = 1×10^{15} ions/cm^2 .

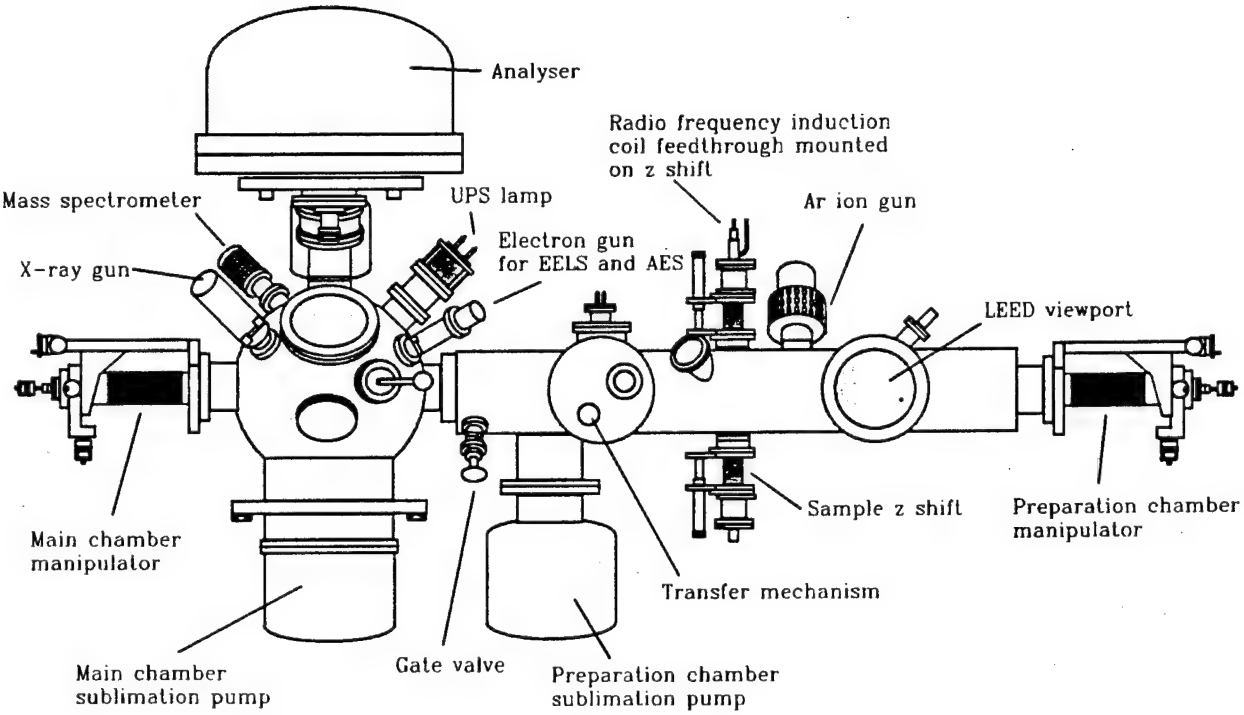

Figure 3.

Schematic representation of the Vacuum Generators Escalab Mark II, which was used to obtain all XPS data.

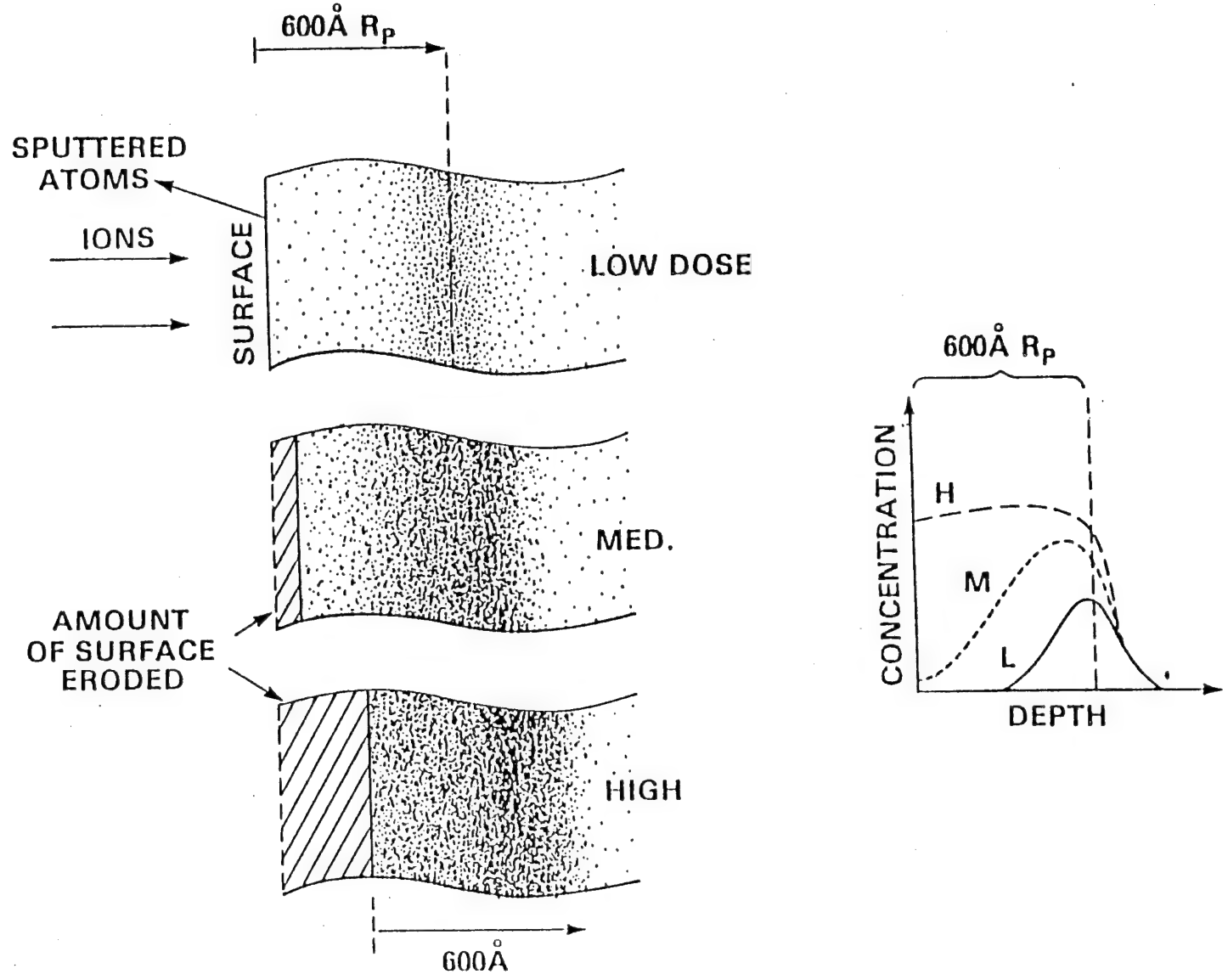

Figure 4.

Schematic view of the depth profile of implanted species as a result of low, medium and high doses. R_p denotes the projected range of the implanted species.

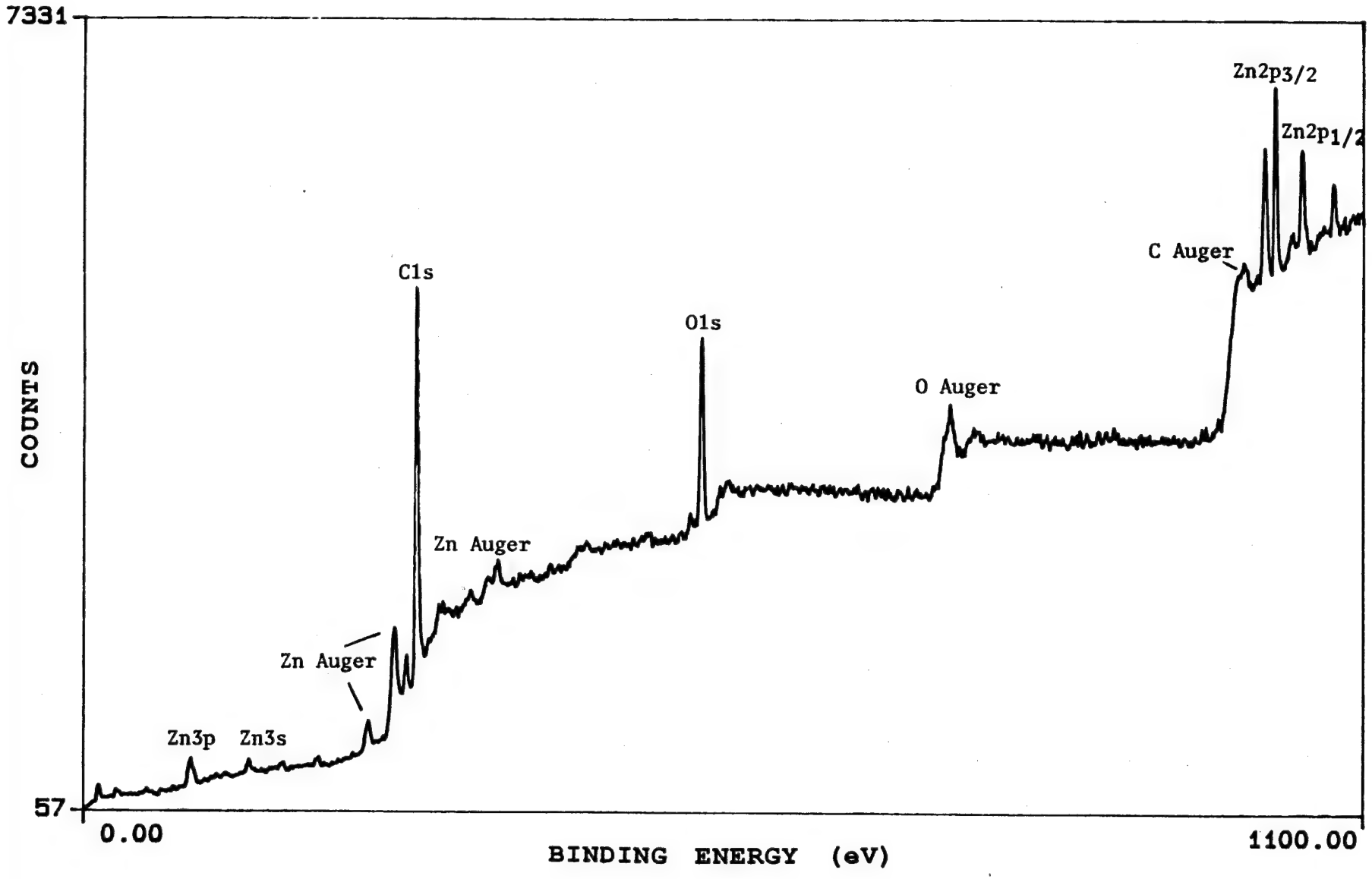

Figure 5.

XPS survey scan of an unimplanted ZnO crystal specimen (Mg Kα).

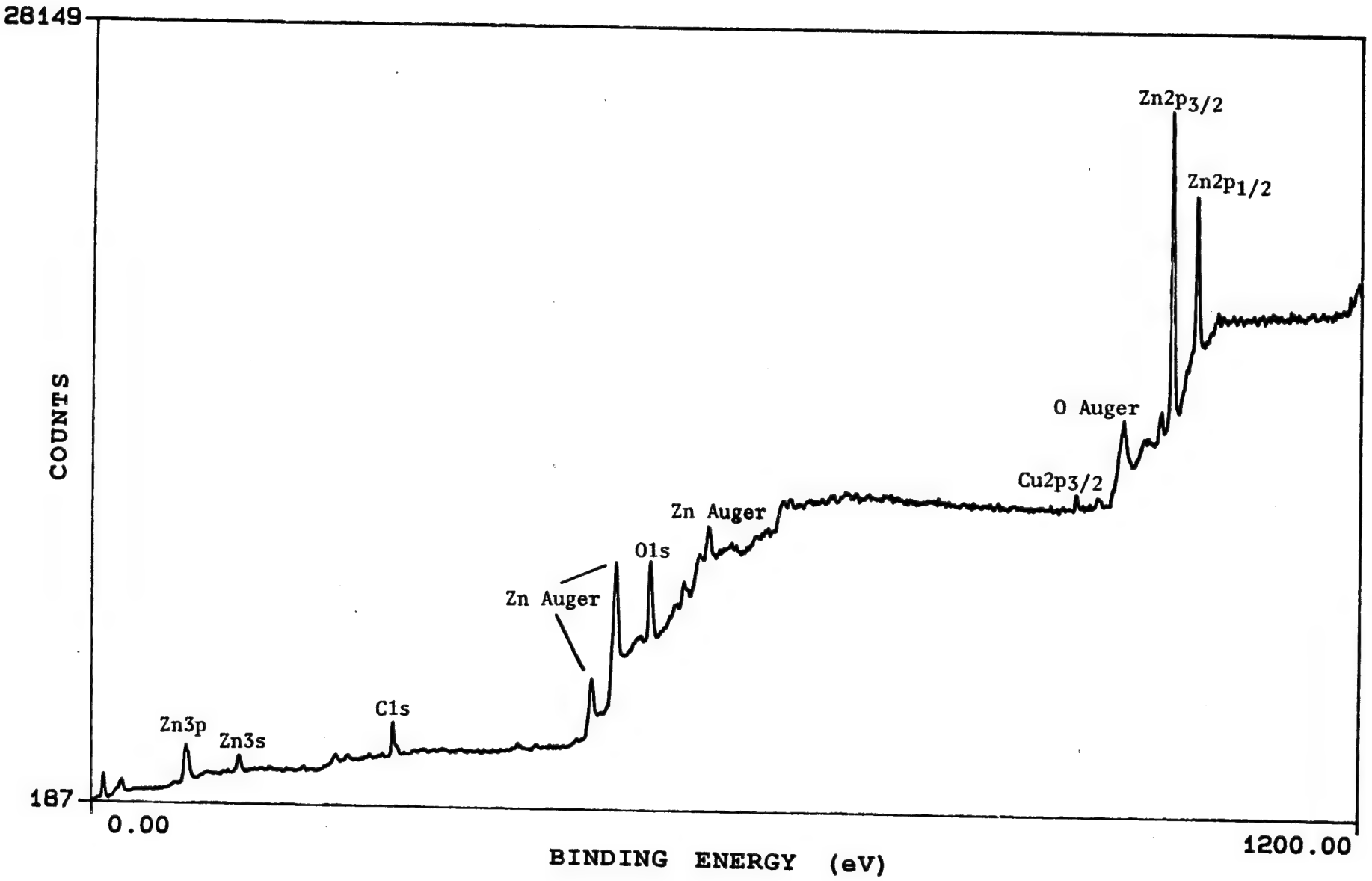

Figure 6.

XPS survey scan of a ^{63}Cu-implanted ZnO single crystal specimen (Al Kα).

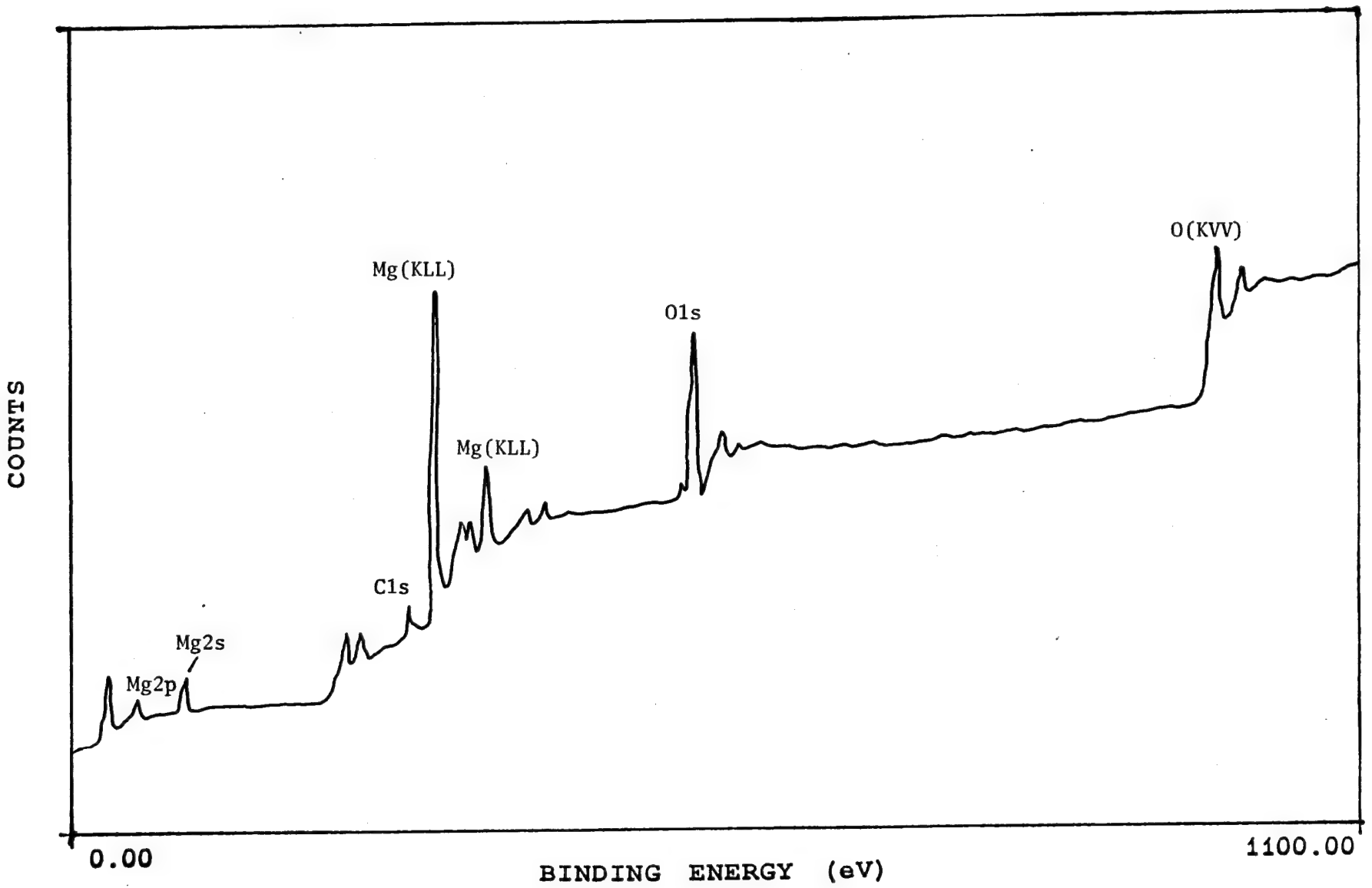

Figure 7.

XPS survey scan of a ^{63}Cu-implanted MgO crystal specimen (Al Kα).

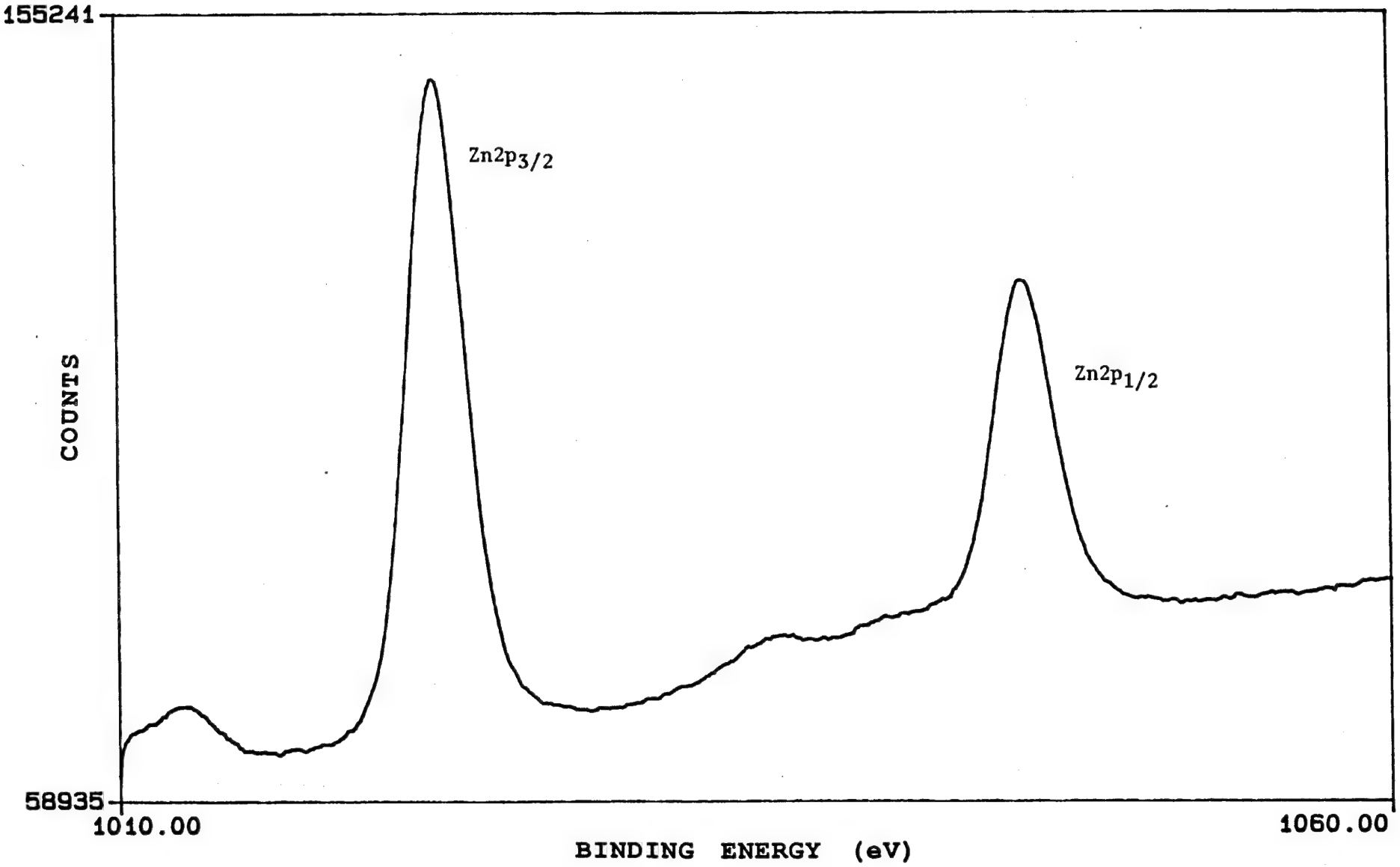

Figure 8.

XPS detail elemental scan (Zn region) of a ^{63}Cu-implanted ZnO crystal specimen (Al Kα).

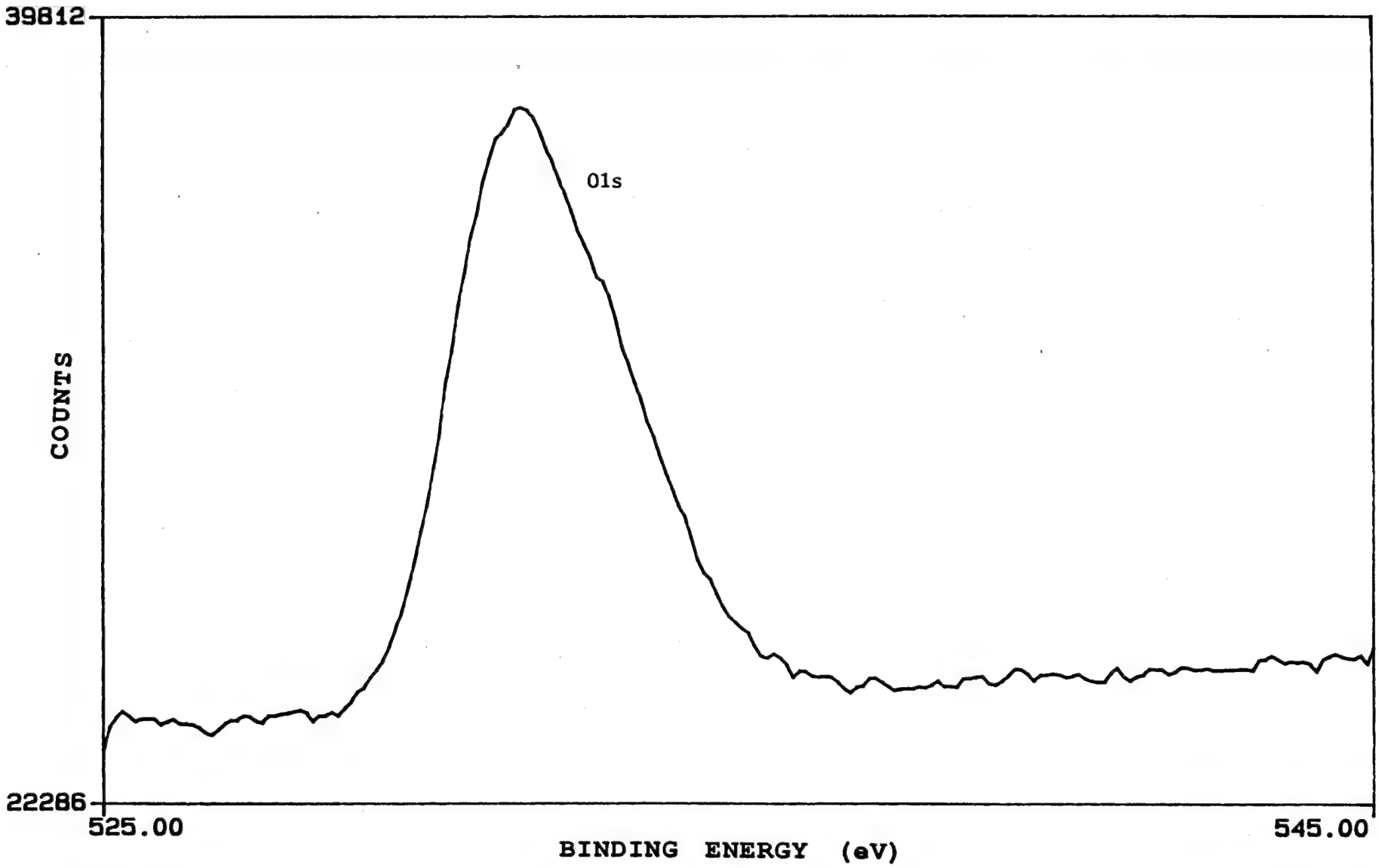

Figure 9.

XPS detail elemental scan (Oxygen region) of a Cu-implanted ZnO single crystal specimen (Al Kα).

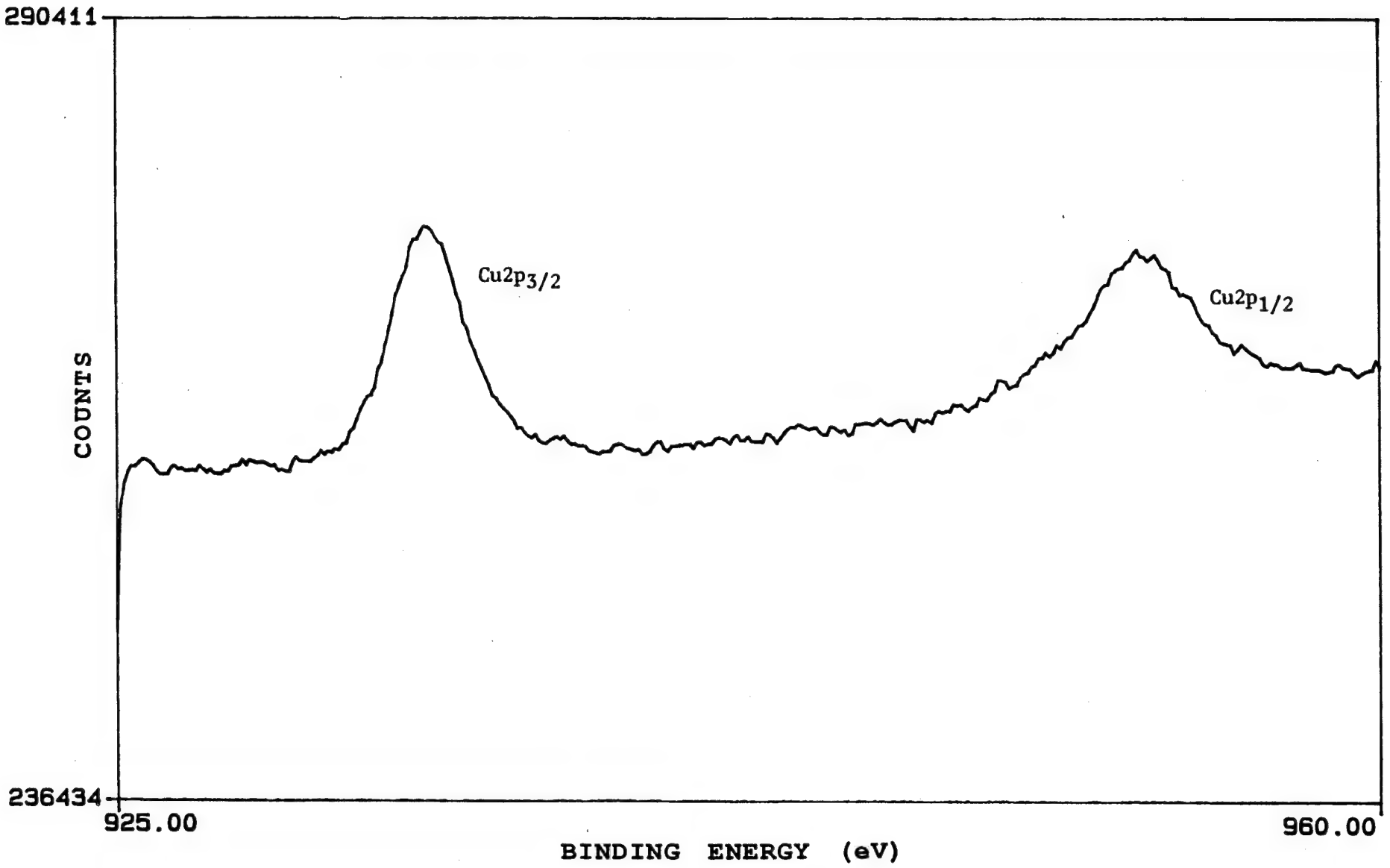

Figure 10.

XPS detail elemental scan (Cu region) of a Cu-implanted ZnO crystal specimen (Al Kα).

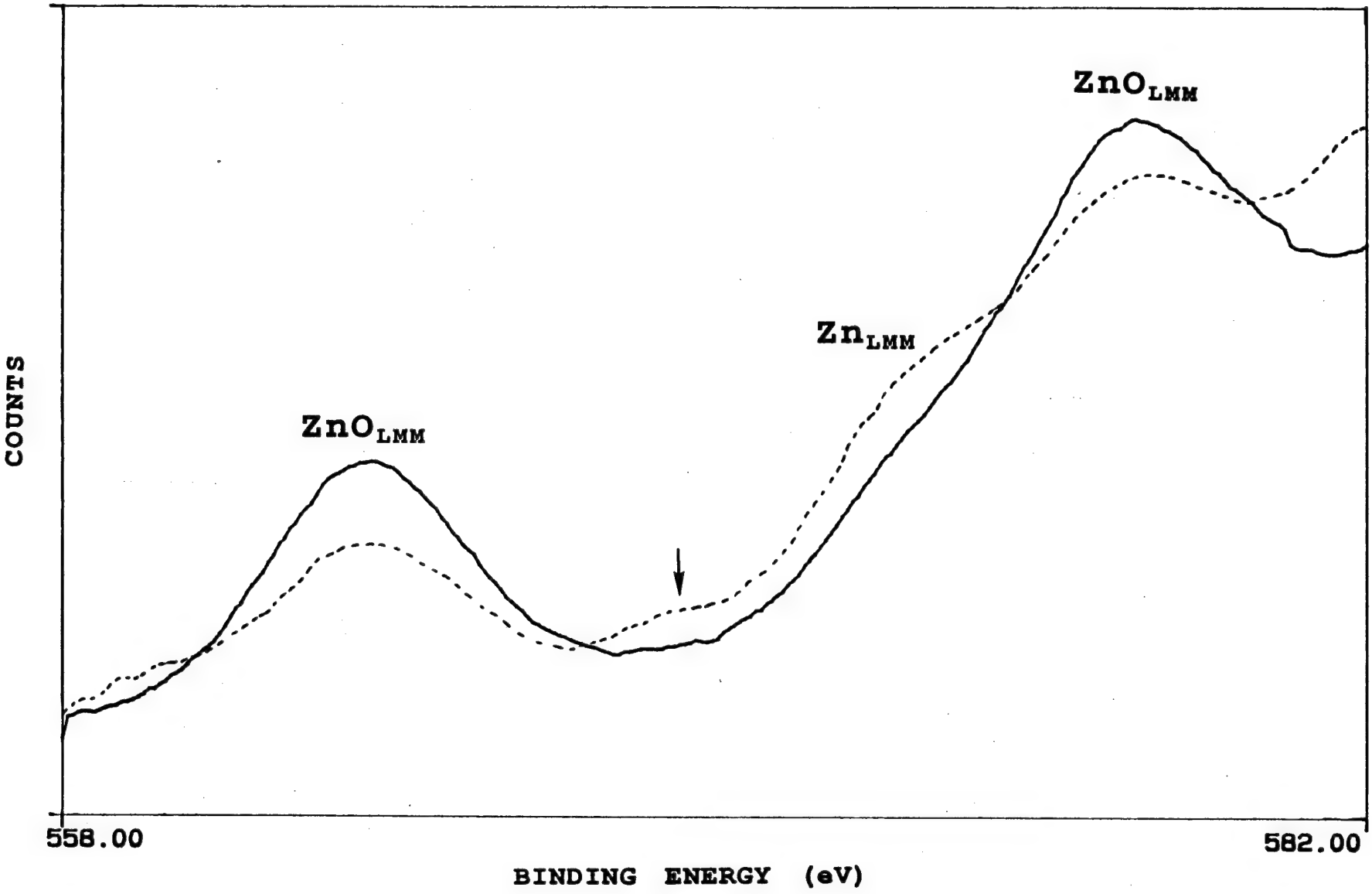

Figure 11.

XPS detail elemental scan (Cu Auger region) of a Cu-implanted ZnO/Zn foil specimen (Al Kα). The broken line is the spectrum of the high dose sample; the solid line is the spectrum of the medium dose sample. Arrow indicates the probable location of the Cu Auger line, which is only apparent in the high dose specimen.

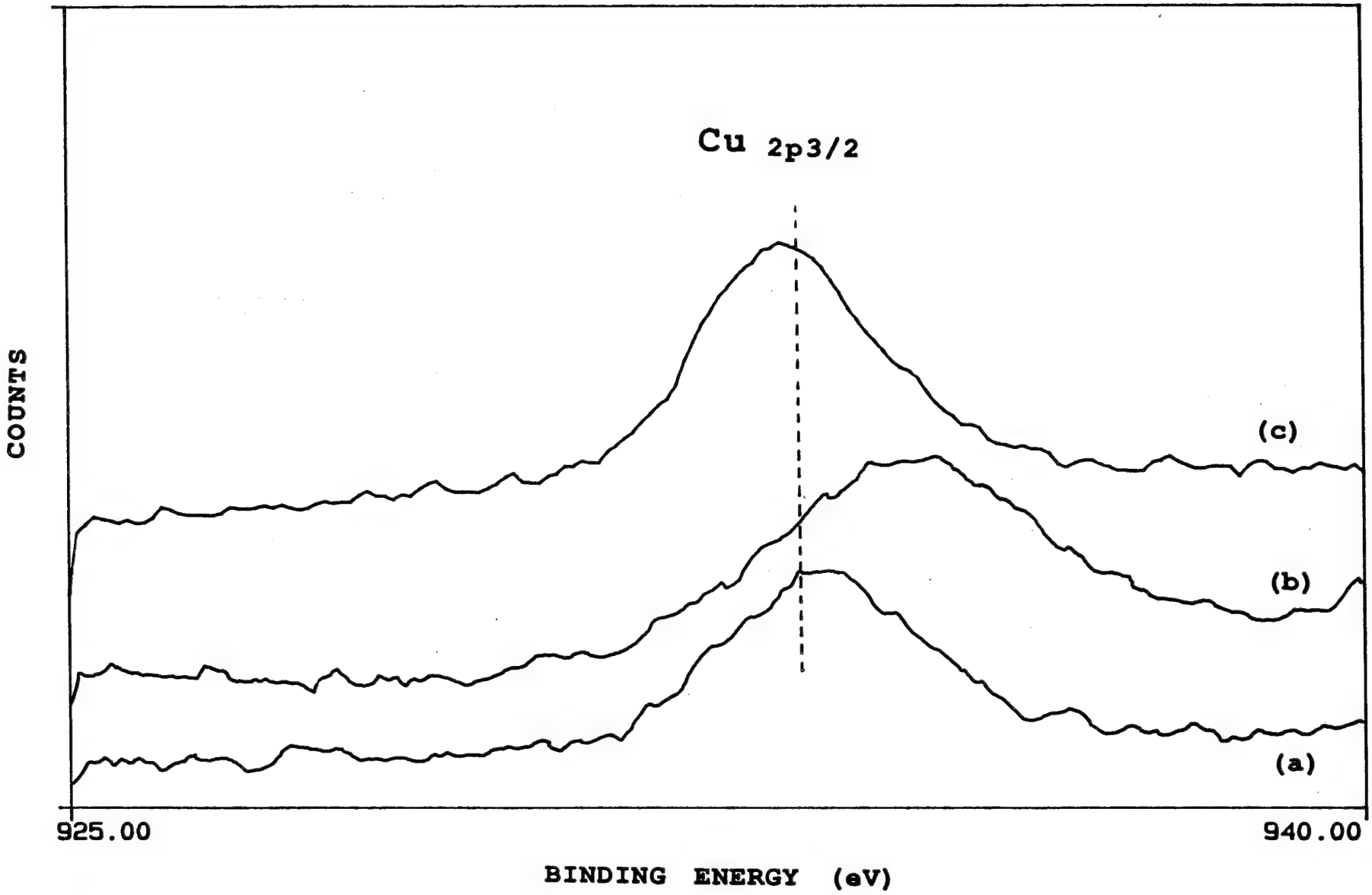

Figure 12.

XPS detail elemental scan (Cu region) of a Cu-implanted ZnO crystal specimen (1988 implantation, Al Kα). (a) before treatment. (b) after heating in oxygen atmosphere. (c) after heating in hydrogen atmosphere.

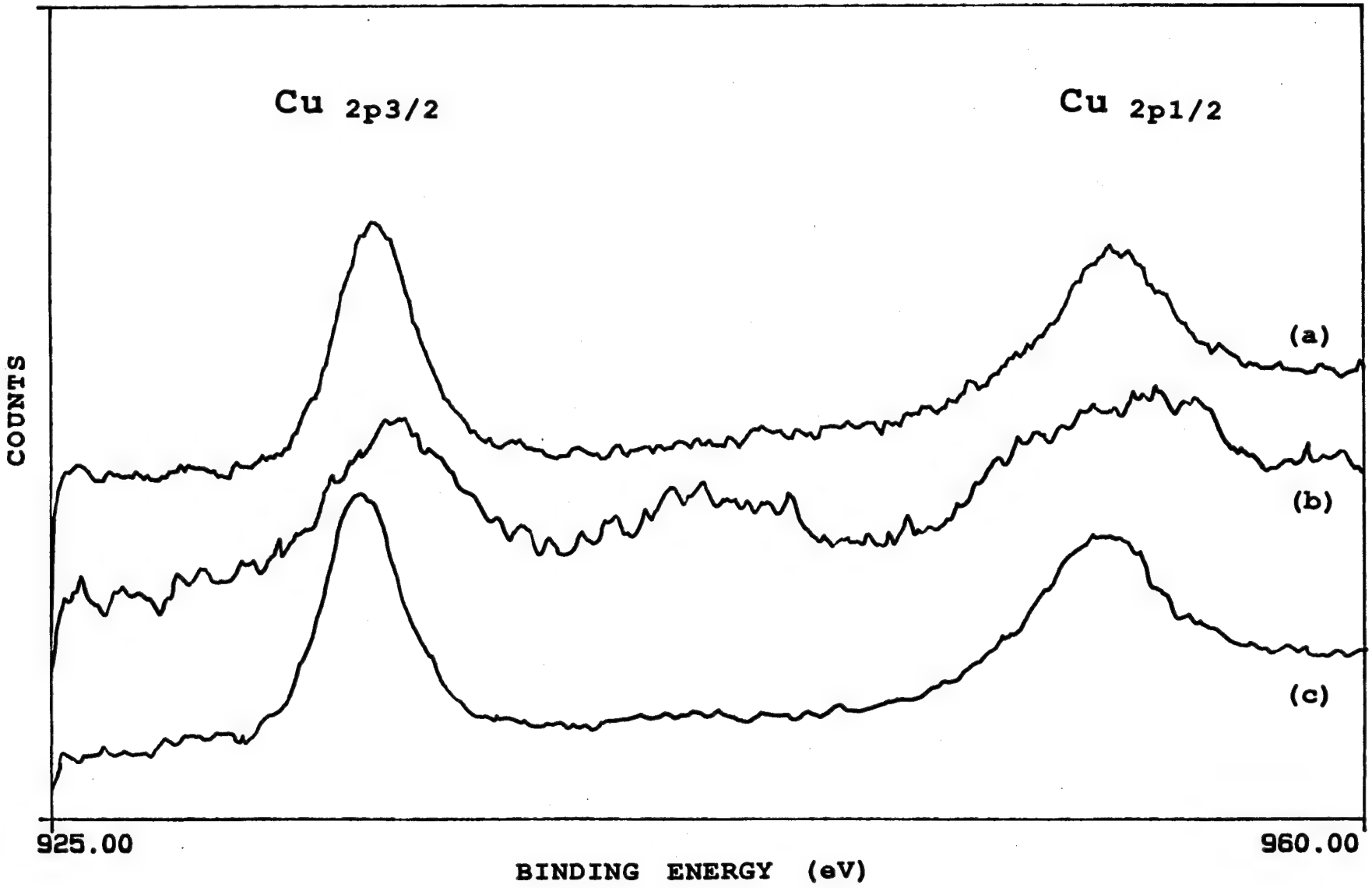

Figure 13.

XPS detail elemental scan (Cu region) of a Cu-implanted ZnO crystal specimen (1988 implantation, Al Kα). (a) before treatment. (b) after heating in oxygen atmosphere. (c) after heating in hydrogen atmosphere.

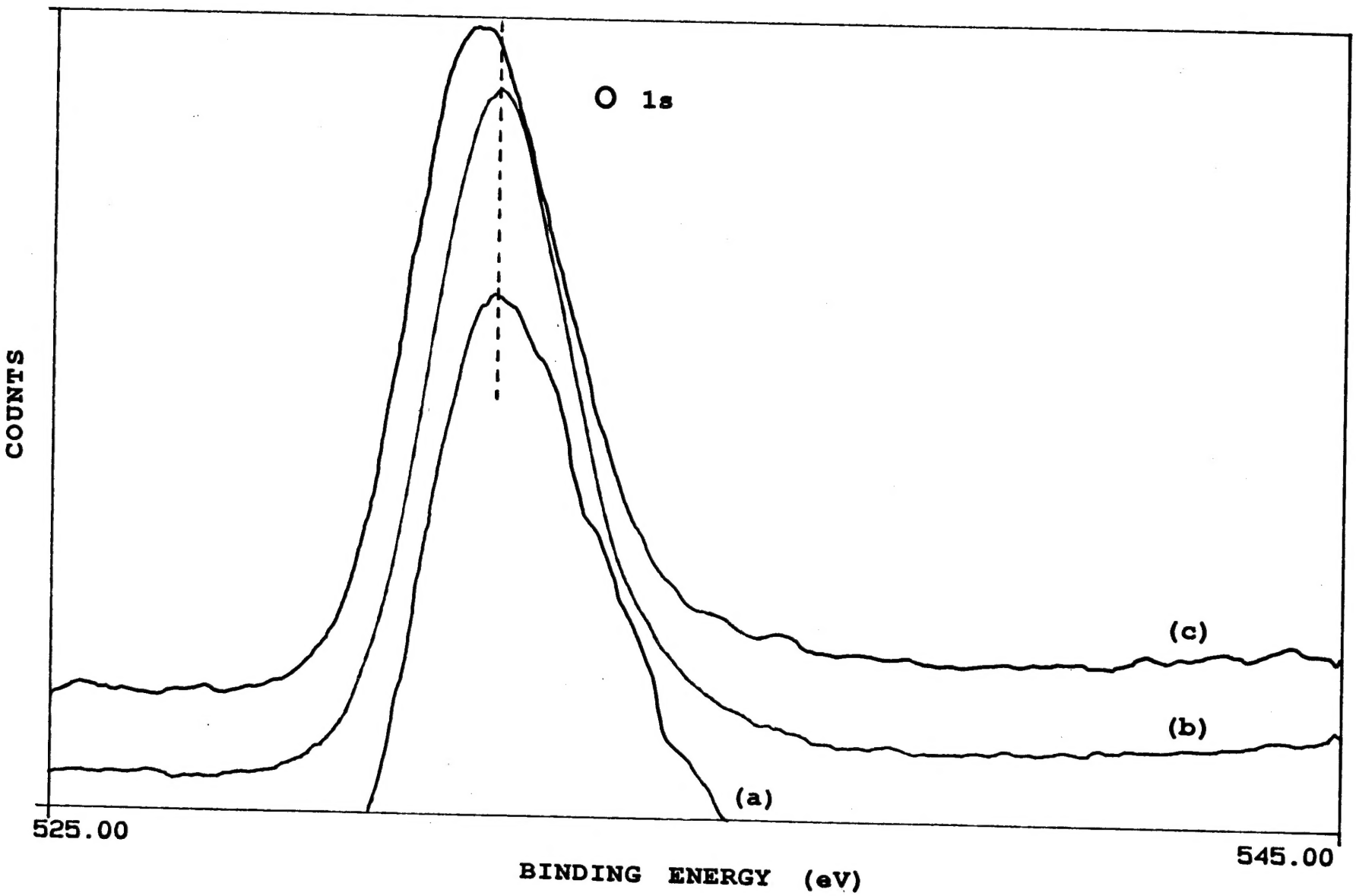

Figure 14.

XPS detail elemental scan (Oxygen region) of a Cu-implanted ZnO crystal specimen (1988 implantation, Al Kα). (a) before treatment. (b) after heating in oxygen atmosphere. (c) after heating in hydrogen atmosphere.

DISTRIBUTION LIST

No. of Copies	To
1	Office of the Under Secretary of Defense for Research and Engineering, The Pentagon, Washington, DC 20301
	Director, U.S. Army Research Laboratory, 2800 Powder Mill Road, Adelphi, MD 20783-1197
1	ATTN: AMSRL-OP-SD-TP, Technical Publishing Branch
1	AMSRL-OP-SD-TA, Records Management
1	AMSRL-OP-SD-TL, Technical Library
	Commander, Defense Technical Information Center, Cameron Station, Building 5, 5010 Duke Street, Alexandria, VA 23304-6145
2	ATTN: DTIC-FDAC
1	MIA/CINDAS, Purdue University, 2595 Yeager Road, West Lafayette, IN 47905
	Commander, Army Research Office, P.O. Box 12211, Research Triangle Park, NC 27709-2211
1	ATTN: Information Processing Office
	Commander, U.S. Army Materiel Command, 5001 Eisenhower Avenue, Alexandria, VA 22333
1	ATTN: AMCSCI
1	AMCMI-IS-A
	Commander, U.S. Army Materiel Systems Analysis Activity, Aberdeen Proving Ground, MD 21005
1	ATTN: AMXSY-MP, H. Cohen
	Commander, U.S. Army Missile Command, Redstone Arsenal, AL 35809
1	ATTN: AMSMI-RD-CS-R/Doc
	Commander, U.S. Army - ARDEC, Information Research Center, Picatinny Arsenal, NJ 07806-5000
1	ATTN: AMSTA-AR-IMC, Bldg. 59
	Commander, U.S. Army Natick Research, Development and Engineering Center Natick, MA 01760-5010
1	ATTN: SATNC-MI, Technical Library
1	SATNC-AI
	Commander, U.S. Army Satellite Communications Agency, Fort Monmouth, NJ 07703
1	ATTN: Technical Document Center
	Commander, U.S. Army Tank-Automotive Command, Warren, MI 48397-5000
1	ATTN: AMSTA-ZSK
1	AMSTA-TSL, Technical Library
1	AMSTA-SF
	President, Airborne, Electronics and Special Warfare Board, Fort Bragg, NC 28307
1	ATTN: Library

No. of Copies	To
	Director, U.S. Army Research Laboratory, Weapons Technology, Aberdeen Proving Ground, MD 21005-5066
1	ATTN: AMSRL-WT
2	Technical Library
	Commander, Dugway Proving Ground, UT 84022
1	ATTN: Technical Library, Technical Information Division
	Commander, U.S. Army Research Laboratory, 2800 Powder Mill Road, Adelphi, MD 20783
1	ATTN: AMSRL-SS
	Director, Benet Weapons Laboratory, LCWSL, USA AMCCOM, Watervliet, NY 12189
1	ATTN: AMSMC-LCB-TL
1	AMSMC-LCB-R
1	AMSMC-LCB-RM
1	AMSMC-LCB-RP
	Commander, U.S. Army Foreign Science and Technology Center, 220 7th Street, N.E., Charlottesville, VA 22901-5396
3	ATTN: AIFRTC, Applied Technologies Branch, Gerald Schlesinger
	Commander, U.S. Army Aeromedical Research Unit, P.O. Box 577, Fort Rucker, AL 36360
1	ATTN: Technical Library
	U.S. Army Aviation Training Library, Fort Rucker, AL 36360
1	ATTN: Building 5906-5907
	Commander, U.S. Army Agency for Aviation Safety, Fort Rucker, AL 3636
1	ATTN: Technical Library
	Commander, Clarke Engineer School Library, 3202 Nebraska Ave., N., Fort Leonard Wood, MO 65473-5000
1	ATTN: Library
	Commander, U.S. Army Engineer Waterways Experiment Station, P.O. Box 631, Vicksburg, MS 39180
1	ATTN: Research Center Library
	Commandant, U.S. Army Quartermaster School, Fort Lee, VA 23801
1	ATTN: Quartermaster School Library
	Naval Research Laboratory, Washington, DC 20375
1	ATTN: Code 6384
	Chief of Naval Research, Arlington, VA 22217
1	ATTN: Code 471
	Commander, U.S. Air Force Wright Research and Development Center, Wright-Patterson Air Force Base, OH 45433-6523
1	ATTN: WRDC/MLLP, M. Forney, Jr.
1	WRDC/MLBC, Mr. Stanley Schulman

No. of Copies	To
	U.S. Department of Commerce, National Institute of Standards and Technology, Gaithersburg, MD 20899
1	ATTN: Stephen M. Hsu, Chief, Ceramics Division, Institute for Materials Science and Engineering
1	Committee on Marine Structures, Marine Board, National Research Council, 2101 Constitution Avenue, N.W., Washington, DC 20418
1	Materials Sciences Corporation, Suite 250, 500 Office Center Drive, Fort Washington, PA 19034
1	Charles Stark Draper Laboratory, 555 Technology Square, Cambridge, MA 02139
	General Dynamics, Convair Aerospace Division, P.O. Box 748, Fort Worth, TX 76101
1	ATTN: Mfg. Engineering Technical Library
	Plastics Technical Evaluation Center, PLASTEC, ARDEC, Bldg. 355N, Picatinny Arsenal, NJ 07806-5000
1	ATTN: Harry Pebly
1	Department of the Army, Aerostructures Directorate, MS-266, U.S. Army Aviation R&T Activity - AVSCOM, Langley Research Center, Hampton, VA 23665-5225
1	NASA - Langley Research Center, Hampton, VA 23665-5255
	U.S. Army Vehicle Propulsion Directorate, NASA Lewis Research Center, 2100 Brookpark Road, Cleveland, OH 44135-3191
1	ATTN: AMSRL-VP
	Director, Defense Intelligence Agency, Washington, DC 20340-6053
1	ATTN: PAQ-4B (Dr. Kenneth Crelling)
	U.S. Army Communications and Electronics Command, Fort Monmouth, NJ 07703
1	ATTN: Technical Library
	U.S. Army Research Laboratory, Electronic Power Sources Directorate, Fort Monmouth, NJ 07703
1	ATTN: Technical Library
	Director, U.S. Army Research Laboratory, Watertown, MA 02172-0001
2	ATTN: AMSRL-OP-WT-IS, Technical Library
5	Author